**Annales
Geophysicae**

The presence of large sunspots near the central solar meridian at the times of major geomagnetic storms

D. M. Willis[1,2], **R. Henwood**[3], **and F. R. Stephenson**[4]

[1]Space Science and Technology Department, Rutherford Appleton Laboratory, Chilton, Didcot, Oxfordshire OX11 0QX, UK
[2]Centre for Fusion, Space and Astrophysics, Department of Physics, University of Warwick, Coventry CV4 7AL, UK
[3]UK Solar System Data Centre, Rutherford Appleton Laboratory, Chilton, Didcot, Oxon OX11 0QX, UK
[4]Department of Physics, University of Durham, Durham DH1 3LE, UK

Abstract. A further study is made of the validity of a technique developed by the authors to identify historical occurrences of intense geomagnetic storms, which is based on finding approximately coincident observations of sunspots and aurorae recorded in East Asian histories. Previously, the validity of this technique was corroborated using scientific observations of aurorae in Japan during the interval 1957–2004 and contemporaneous white-light images of the Sun obtained by the Royal Greenwich Observatory, the Big Bear Solar Observatory, the Debrecen Heliophysical Observatory, and the Solar and Heliospheric Observatory spacecraft. The present investigation utilises a list of major geomagnetic storms in the interval 1868–2008, which is based on the magnitude of the *AA*∗ magnetic index, and reconstructed solar images based on the sunspot observations acquired by the Royal Greenwich Observatory during the shorter interval 1874–1976. It is found that a sunspot large enough to be seen with the unaided eye by an "experienced" observer was located reasonably close to the central solar meridian for almost 90% of these major geomagnetic storms. Even an "average" observer would easily achieve a corresponding success rate of 70% and this success rate increases to about 80% if a minority of ambiguous situations are interpreted favourably. The use of information on major geomagnetic storms, rather than modern auroral observations from Japan, provides a less direct corroboration of the technique for identifying historical occurrences of intense geomagnetic storms, if only because major geomagnetic storms do not necessarily produce auroral displays over East Asia. Nevertheless, the present study provides further corroboration of the validity of the original technique for identifying intense geomagnetic

storms. This additional corroboration of the original technique is important because early unaided-eye observations of sunspots and aurorae provide the only possible means of identifying individual geomagnetic storms during the greater part of the past two millennia.

1 Introduction

The validity of a technique developed by Willis et al. (2005) to identify historical occurrences of intense geomagnetic storms, which is based on finding approximately coincident observations of sunspots and aurorae recorded in East Asian histories, has been corroborated using more modern sunspot and auroral observations. In particular, Willis et al. (2006) used scientific observations of aurorae in Japan during the interval 1957–2004 (Shiokawa et al., 2005) to identify geomagnetic storms that are sufficiently intense to produce auroral displays at low geomagnetic latitudes. By examining white-light images of the Sun obtained by the Royal Greenwich Observatory (RGO), the Big Bear Solar Observatory (BBSO), the Debrecen Heliophysical Observatory (DHO) and the Solar and Heliospheric Observatory (SOHO) spacecraft, it was found that at least one sunspot large enough to be seen with the unaided eye by an "experienced" observer was located reasonably close to the central solar meridian immediately before all but one of the 30 distinct Japanese auroral events in the interval 1957–2004; this represents a 97% success rate. Even an "average" observer would probably have been able to see at least one sunspot with the unaided eye before 24 of these 30 events, which represents

an 80% success rate. As noted by Willis et al. (2006), this corroboration of the validity of the technique used to identify historical occurrences of intense geomagnetic storms (Willis et al., 2005) is important because early unaided-eye observations of sunspots and aurorae provide the only possible means of identifying individual geomagnetic storms during the greater part of the past two millennia. Indeed, this identification of geomagnetic storms is only feasible because the dates of many unaided-eye observations of sunspots and aurorae during the last 2000 years are known precisely (year, month and day all recorded exactly). Conversely, the radioisotopes ^{14}C and ^{10}Be, which are extremely valuable in studies of long-term variations in solar activity, have a time resolution of at least several weeks and hence these radioisotopes cannot be used to identify historical occurrences of individual geomagnetic storms.

The historical sunspot observations from East Asia extend throughout the interval 165 BC–AD 1918 (Willis et al., 2005), although a significant proportion of the early sunspot observations do not have precise dates (i.e. year, month and day are not all recorded exactly). Similarly, the historical auroral observations from East Asia extend throughout the interval 210 BC–AD 1911, although in this case many of the early auroral observations and also the single observation in AD 1911 do not have precise dates. The modern Japanese auroral observations used to validate the technique employed in the identification of historical occurrences of intense geomagnetic storms (Willis et al., 2006) lie within the much shorter interval AD 1957–2004. However, the great merit of using modern Japanese auroral observations is that these observations are from the same region of the World as the historical auroral observations (China, Japan and Korea). The purpose of the present paper is to investigate further the validity of the technique used to identify historical occurrences of intense geomagnetic storms, utilising a list of "modern" geomagnetic storms in the interval AD 1868–2008 that is based on the AA^* magnetic index (Allen, 1982; Coffey and Erwin, 2001). The term "modern" is used here as a convenient converse of the term "historical".

An investigation of the presence of large sunspots near the central solar meridian at the times of modern geomagnetic storms provides a slightly less direct validation of the technique used to identify historical occurrences of intense geomagnetic storms, at least in the sense that not all geomagnetic storms identified by the AA^* magnetic index necessarily generate auroral displays that are visible in East Asia. However, the geomagnetic storms identified by the AA^* magnetic index extend over a period of time (AD 1868–2008) that overlaps, albeit briefly, the much longer period of historical auroral and sunspot observations from East Asia. Comparisons between the magnetic and sunspot data are restricted to the shorter interval AD 1874–1976 because this study is based specifically on the Royal Greenwich Observatory (RGO) routine programme of sunspot observations, which began in 1874 and ceased at the end of December in 1976.

The method employed in this paper follows closely that developed by Willis et al. (2006). However, the method has to be partly automated because of the large number (1074) of major geomagnetic storms in the interval 1874 April 17– 1976 December 31. In particular, it is impracticable to show all the solar images for the six-day intervals immediately before these major storms, contrary to the situation in the paper by Willis et al. (2006), so statistical results have to be presented instead. The main statistical results, which are given in Table 2, are discussed in Sect. 5. However, two figures similar to those published by Willis et al. (2006) are presented in Sect. 6 to clarify the semi-automatic procedure for identifying sunspots large enough to be seen with the unaided eye by "average" and "experienced" sunspot observers. The main conclusions are summarised briefly in Sect. 7.

2 Geomagnetic storms defined by the AA^* magnetic index

In this study, the definition of a geomagnetic storm is based on the aa magnetic index, which has been calculated retrospectively from the year 1868 (Mayaud, 1972, 1973, 1980). This index is defined by the average, for each 3-h interval, of the K magnetic indices from two near-antipodal observatories after the transformation of these indices into amplitudes (nT). The two antipodal observatories used to form the aa index were initially Greenwich (1868–1925) and Melbourne (1868–1919). In the Northern Hemisphere, the observations at Greenwich were continued first at Abinger (1926–1956) and subsequently at Hartland (1957–present): in the Southern Hemisphere, the observations at Melbourne were continued first at Toolangi (1920–1979) and then at Canberra (1980–present).

At each change of observatory, a site correction was made for changes in geomagnetic latitude and local induction effects (Mayaud, 1972, 1973, 1980; Clilverd et al., 2005; Svalgaard and Cliver, 2007). In the case of the northern observatory, this was achieved by performing the K-index scalings for two years at a neighbouring observatory (for times before and after the change of site), in order to estimate the calibration that is required to equalise the annual means of the old and new observatories (Mayaud, 1973, 1980). In the case of the southern observatory, no neighbouring observatory was available and hence the normalisation was performed with respect to the normalised series for the northern observatory. However, it has been claimed by Svalgaard and Cliver (2007) that the observed annual means of the aa index before the year 1957 are too small by about 3 nT, compared with values calculated from the inter-hourly variability (IHV) index of geomagnetic activity (Svalgaard et al., 2004). Svalgaard and Cliver (2007) interpret this discrepancy as an indication that the calibration of the aa index is incorrect before 1957 (see also Jarvis, 2005; Mursula and Martini, 2006; Rouillard et al., 2007). Nevertheless, an increase of about 3 nT in aa

(and hence in $AA*$) is unlikely to be critical in the identification of major geomagnetic storms. To remove local diurnal ionospheric effects, 8-point running means of aa are calculated to generate (running) 24-h average values, which are denoted here by the symbol $AA*$ (upper case letters are used to indicate 24-h averages of eight three-hourly aa indices). The $AA*$ magnetic index yields the largest 24-h running average during the course of a geomagnetic storm, denoted here by $AA*$(max), which is derived independently of the start and end times (UT) of the day.

Different definitions of a geomagnetic storm have been propounded in terms of the magnitude of the $AA*$ magnetic index. For example, in the investigation by Clilverd et al. (1998) a geomagnetic storm was identified as beginning when $AA* \geq 40$ nT and was considered to end when $AA*$ drops below 40 nT for two consecutive 3-h intervals. In the present study, a major geomagnetic storm is defined to begin when $AA* > 60$ nT and is considered to remain in progress until $AA* < 60$ nT. The reasons for using this particular definition of a major geomagnetic storm are twofold. First, a digital list of major geomagnetic storms in the interval AD 1868–2008 (the list currently extends up to March 2008) that satisfy these particular criteria already exists (ftp://ftp.ngdc.noaa.gov/STP/GEOMAGNETIC_DATA/AASTAR/aastar.lst.v7). Second, it seems logical to consider major modern geomagnetic storms in any attempt to justify the validity of the technique used by Willis et al. (2005) to identify historical occurrences of intense geomagnetic storms using combined sunspot and auroral observations from East Asia (China, Japan and Korea). In this latter context, it should be noted that many of the modern low-latitude aurorae observed in Japan do indeed occur during intense (or major) geomagnetic storms, as measured by the D_{st} index (Shiokawa et al., 2005). It should also be noted briefly that the $Ap*$ magnetic index has some advantages over the $AA*$ magnetic index in certain circumstances (Coffey and Erwin, 2001) but the former index is only available from 1932. However, there is no systematic discrepancy between the observed and calculated values of ap, and hence $Ap*$, contrary to the discrepancy ($\cong 3$ nT) for the aa index (Svalgaard and Cliver, 2007).

The digital list of major geomagnetic storms defined by the $AA*$ magnetic index provides the following tabulated information: the start date of the onset of the condition $AA* > 60$ nT; the start time (UT) of the onset of this condition (i.e. the start time of the appropriate 3-h interval); the date on which $AA*$ attains its maximum value, denoted by $AA*$(max); the start time (UT) of the 3-h interval during which this maximum is attained; the end date of the storm; the start time (UT) of the 3-h interval defining the end of the storm (i.e. the onset of $AA* < 60$ nT); the duration of the storm in hours; the numerical value of $AA*$(max); the average numerical value of $AA*$ during the course of the storm, denoted by $AA*$(avg); and the sum of the 3-hourly aa indices throughout the storm (i.e. $\Sigma\, aa$). Since aa is defined for 3-h

intervals, it should be noted that both the start and end times (UT) of a major geomagnetic storm are defined with respect to the beginning of a 3-h interval and hence the duration of the storm is defined as the end time – the start time +3 h. The only tabulated data used in the present paper are the start date and onset time (UT) of each major geomagnetic storm.

3 The Royal Greenwich Observatory sunspot data

The sunspot data used in this investigation are based entirely on the white-light solar observations maintained and organised for more than a century by the Royal Greenwich Observatory (RGO). Newton (1958) and Howse (1975) have published detailed descriptions of the photoheliographs used in this programme of solar observations and the paper by Willis et al. (1996) provides further details of the method of extracting sunspot information from the solar photographs. The measured values of sunspot areas and positions, derived from the solar photographs, have been archived as the "Greenwich Photo-heliographic Results, 1874–1976" (Greenwich Observations, 1874–1955; Royal Observatory Bulletins, Series C, 1956–1961; Royal Observatory Annals, 1962–1976). These RGO publications provide tabulations of the measured positions and areas (both umbral areas and umbral plus penumbral areas) of every sunspot group for most days of the year. The measured projected areas are corrected for foreshortening and then expressed in millionths of the Sun's visible hemisphere.

In the earlier discussion of the presence of large sunspots near the central solar meridian at the times of modern Japanese auroral observations (Willis et al., 2006), use was also made of white-light images of the Sun acquired by the Big Bear Solar Observatory (BBSO), the Debrecen Heliophysical Observatory (DHO) and the Solar and Heliospheric Observatory (SOHO) spacecraft. The inclusion of this additional solar information was essential for comparisons with modern Japanese auroral observations in the interval 1957–2004. In the present study, however, the discussion is deliberately restricted to the Royal Greenwich Observatory (RGO) sunspot observations in the interval 1874–1976. Although the RGO solar photographs were actually acquired at several different observatories (Willis et al., 1996), the determination of the sunspot positions and areas was performed to a common standard. Therefore, the RGO solar observations constitute an essentially homogeneous dataset throughout the interval 1874–1976. Following the closure of the RGO programme of solar observations at the end of 1976, the homogeneity of the extended dataset is at least questionable. Indeed, specific reservations have been expressed about the continued homogeneity of the dataset in the years immediately after 1976 (Foster, 2004). Nevertheless, the present study could easily be extended up to 2008 (currently the $AA*$ list of major geomagnetic storms extends up to March 2008) once a reliable and homogeneous digital dataset is available

for the entire interval 1874–2008. However, it seems unlikely that the inclusion of additional data for the interval 1977–2008 would alter the main conclusions of this paper.

A digital dataset that contains the sunspot positions and areas published (in printed form) by the RGO was distributed many years ago by World Data Center A, Boulder, Colorado. This original dataset has been used in the present investigation because the projected sunspot areas are given explicitly and do not have to be re-derived from the corrected sunspot areas. However, a more detailed digital dataset, which also includes facular positions and areas, has subsequently been prepared under the auspices of the NOAA National Geophysical Data Center (NGDC), Boulder, Colorado. This second dataset has been of slightly more limited value to the scientific community because, in its original form, it did not contain digital data for a few of the earlier years. At the inception of the NGDC project, the relevant RGO printed publications for the interval 1878–1885 were not immediately available but this omission has since been rectified by the inclusion of digital data prepared separately by a contractor sponsored by an individual scientist. It must be conceded, however, that neither digital dataset (either with or without facular information) has yet been subjected to the most rigorous tests in terms of quality assurance. Indeed, it is known that both digital datasets definitely contain errors. More specifically, it is known that during the early years (before about 1918) the position of a sunspot sometimes appears to change anomalously (or discontinuously) in the original digital dataset, which only contains sunspot information. Such "anomalies" occur in the projected co-ordinates, namely radial distance and polar angle, but not in the heliographic co-ordinates, namely heliographic latitude and longitude. Similarly, there are some typographical errors in the second dataset containing facular data, particularly during the (initially) "missing" years (1878–1885). Procedures are now being implemented to correct both digital datasets.

Rather than provide a long and discursive discussion on the provenance and accuracy of the two digital datasets, the policy adopted in this study is to check visually the positions of all sunspots on the solar disk (in both projected and heliographic co-ordinates) for the relevant six days preceding each of the 1074 major geomagnetic storms in the interval 1874–1976. This visual check is achieved by displaying sequentially on a monitor the appropriate daily reconstructed solar images, using the reconstruction technique developed by Willis et al. (1996); see Sect. 4 for further details of this reconstruction process. A semi-automatic procedure has been developed to examine these daily solar images, in order to ensure that in the early years a minority of anomalous (or discontinuous) changes of sunspot position in the original digital dataset (in just the projected co-ordinates) does not invalidate any of the conclusions of this paper. It must be emphasised, however, that the task of checking the entire digital dataset containing the measured positions and areas of both sunspots and faculae against the printed data in the RGO publications would be an enormous undertaking, which must be deferred at least until a semi-automatic checking and correcting procedure can be developed.

4　Criteria for sunspot visibility with the unaided eye

Following the approach adopted in the study of the presence of large sunspots near the central solar meridian at the times of modern Japanese auroral observations (Willis et al., 2006), the goal in this paper is to consider the size and position of all sunspots on the solar disk from 1 to 6 days before the onset of the major geomagnetic storms defined and discussed in Sect. 2. The time interval over which sunspots are examined is based on the assumption (in the identification of an historical geomagnetic storm) that the time delay between the occurrence of the energetic solar feature producing the geomagnetic storm and the onset of the storm itself lies within the range 1 to 6 days. The shortest known time delay between an energetic solar feature and the onset of a geomagnetic storm is about 17.5 h. This time delay is associated with the first observation of a white-light flare on 1859 September 1 (Carrington, 1860; Hodgson, 1860) and the abrupt onset of a great geomagnetic storm on the following day. Therefore, as in the study of the presence of large sunspots near the central solar meridian at the times of modern Japanese auroral observations (Willis et al., 2006), the six days immediately before the onset of a major geomagnetic storm are defined in such a way that the time of the RGO solar observation on the "first" day before the day of the onset of the geomagnetic storm is as close as possible to, but greater than, this limiting value of 17.5 h.

The sizes of all sunspots on the solar disk can be compared with the threshold size of a sunspot capable of being detected with the unaided eye. As in previous papers (Willis et al., 2005, 2006), a distinction is made between "average" and "experienced" sunspot observers. Specifically, it is assumed that an "average" observer can routinely detect sunspots with umbral and umbral plus penumbral (whole–spot) diameters of 15 and 41 arc s, respectively. However, it seems likely that an "experienced" observer can detect sunspots with a penumbral diameter of about 25 arc s under optimal viewing conditions. Both criteria are used to assess the possibility of detecting a sunspot with the unaided eye (in the absence of cloud cover) before each of the major geomagnetic storms defined in Sect. 2.

In the search for large sunspots near the central solar meridian at the times of modern Japanese auroral observations (Willis et al., 2006), the sizes of sunspots present in white-light images of the Sun were compared with the sizes of the threshold areas for the detection of sunspots with the unaided eye by both "average" and "experienced" observers. However, since there are only 30 distinct Japanese auroral events in the interval 1957–2004, it is quite feasible to present actual solar images for the six-day intervals

Table 1. The characteristic variation of the threshold sunspot areas during the course of the year is exemplified by presenting approximate numerical values of these projected areas for the minimum, mean and maximum distances of the Sun from the Earth. Numerical values of the projected umbral and whole-spot (umbral + penumbral) threshold areas, measured in millionths of the solar disk, are given for both "average" and "experienced" sunspot observers. For brevity, the symbols U_0 and W_0 ($=U_0+P_0$) are used to denote the umbral and whole-spot threshold areas. The uncertainties associated with the threshold areas are based on characteristic uncertainties of $\pm 10\%$ in the threshold sunspot dimensions (see Sects. 4 and 5 for further details); the first and second numbers in [square] parentheses correspond, respectively, to increases and decreases of 10% in the threshold sunspot dimensions quoted in arc seconds. These uncertainties are realistic illustrative "errors", not absolute bounds on the "errors".

Threshold areas (millionths of the Sun's visible disk)			
Umbral (U_0) or Whole-spot (W_0) area	Distance of Sun from Earth		
(average or experienced observer)	Minimum	Mean	Maximum
U_0 (average observer)	59 [+12, −11]	61 [+13, −12]	63 [+13, −12]
W_0 (average observer)	440 [+92, −84]	455 [+96, −86]	470 [+99, −89]
W_0 (experienced observer)	164 [+34, −31]	169 [+36, −32]	175 [+37, −33]

immediately prior to each of these 30 auroral events. Presentation of actual solar images is clearly impracticable for the large number ($>$1000) of major geomagnetic storms in the interval 1874 April 17–1976 December 31. Therefore, the procedure employed previously has to be semi-automated. Although the comparisons between actual sunspot areas and threshold sunspot areas at the times of modern Japanese auroral observations are largely visual, it is obviously possible to quantify the procedure.

Figure 1a in the paper by Willis et al. (2006) shows schematically the threshold areas for the detection of sunspots with the unaided eye for both "average" and "experienced" sunspot observers. This figure is intended to emphasise (at least conceptually) the fact that there is a small variation of these threshold areas during the course of the year. According to the threshold areas quoted previously, Fig. 1a (Willis et al., 2006) shows, alternately, a single sunspot with umbral and umbral plus penumbral diameters of 15 and 41 arc s, located at the centre of the solar disk, and a single sunspot with just a penumbral area of 25 arc s, again located at the centre of the solar disk. The first, second and third pairs of images in this figure (viewed from the left) show sequentially the corresponding threshold areas for "average" and "experienced" observers, respectively, for the minimum, mean and maximum distances of the Sun from the Earth during the course of the year, if all images are reduced to a common solar diameter. Numerical values of these threshold areas are presented in Table 1. Although the annual variation in the semi-diameter of the Sun, as seen from the Earth, makes an undetectable visual difference in the threshold areas (for both "average" and "experienced" observers), at least on the scale of all displayed figures (cf. Willis et al., 2006), this annual variation in the apparent semi-diameter of the Sun is allowed for in the quantitative calculations (Sect. 5). Despite the fact that larger changes in the sunspot threshold areas arise from uncertainties ($\sim$10%) in the threshold sunspot di-

mensions in arc seconds, as discussed in Sect. 5, the changes in threshold sunspot areas associated with annual variations in the apparent semi-diameter of the Sun are still significant.

Moreover, because of foreshortening, the projected threshold areas shown in Fig. 1a of the paper by Willis et al. (2006) would become elliptical and smaller if they were simply rotated away from the centre of the solar disk. Therefore, the true threshold areas of sunspots, which are merely depicted at the centre of the solar disk for convenience, must be used in comparisons with actual sunspot areas, irrespective of the location of the latter on the solar disk.

The condition for the detection of an historical geomagnetic storm is also based on the assumption that the energetic solar feature producing the historical geomagnetic storm must have occurred when the associated sunspot was within ± 4 days (or about $\pm 50°$ of heliographic longitude) of the central solar meridian (Willis et al., 2005). Therefore, in the context of testing the procedure for identifying historical occurrences of geomagnetic storms, using modern observations of sunspots and major geomagnetic storms, a sunspot (or sunspot group) must not only be large enough to be seen with the unaided eye but it must also be within ± 4 days of the central solar meridian. To illustrate this additional criterion, each (reconstructed) solar image in Fig. 1a of the paper by Willis et al. (2006) also shows dotted lines (meridians) at $\pm 50°$ of heliographic longitude with respect to the central meridian. Based on the statistical evidence for an association between the heliographic location of an active solar region and the subsequent onset of a geomagnetic storm (Hudson et al., 1998; Webb et al., 2000; Cane et al., 2000; Berdichevsky et al., 2002; Cane and Richardson, 2003; Srivastava and Venkatakrishnan, 2004; Kim et al., 2005; Gopalswamy et al., 2005, 2007; Schwenn et al., 2005; Kang et al., 2006; Zhang et al., 2007a, b; Tsurutani et al., 2008), sunspot groups that are closer to the central meridian than the dotted lines, and also large enough to be seen with the unaided eye,

are likely to be associated with major geomagnetic storms. Conversely, sunspot groups that are further from the central meridian than the dotted lines are unlikely be associated with major geomagnetic storms, irrespective of their size. In this latter case, the corresponding active solar region (and hence energetic solar feature) is usually too far from the central solar meridian to generate a major geomagnetic storm.

In the search for large sunspots near the central solar meridian at the times of modern Japanese auroral observations (Willis et al., 2006), solar images in the interval 1957–1960 had to be reconstructed from the archived RGO data – using the technique developed previously by Willis et al. (1996) – because it was not possible to obtain digitised images of the original RGO solar plates on a realistic timescale. This reconstruction of solar images is based on the assumption that the umbral and umbral plus penumbral (whole-spot) areas of each sunspot group can be represented by concentric circular areas (or, more accurately, zones of one base) on the visible hemispherical solar surface. The common centre of these two circular areas is supposed to be located at the centre of the sunspot group. This approach allows for foreshortening but is based on the assumption that the boundaries of the observed (i.e. projected) umbral and penumbral areas are exact ellipses. An assumption of this type is an almost inevitable consequence of the fact that no information on the irregular shapes of individual sunspots, and only limited information on the irregular distribution of spots within groups (i.e. a tenfold classification scheme ranging from a single spot to a pair of clusters of spots or a composite group of spots), has been archived in the "Greenwich Photo-heliographic Results, 1874–1976".

The technique for reconstructing solar images forms the basis of a semi-automated search for large sunspots near the central solar meridian at the times of major geomagnetic storms. In practice, the measured sunspot areas are compared with the threshold sunspot areas for the six days immediately before each of the major geomagnetic storms defined in Sect. 2. Conceptually, this approach is the quantitative equivalent of the essentially qualitative comparisons made in the paper by Willis et al. (2006), which compared the threshold areas shown in their Fig. 1a with both actual and reconstructed solar images immediately before modern Japanese auroral observations. The results were presented as a sequence of solar images on the relevant six days immediately before the 30 distinct auroral events and the visual comparisons were performed for both "average" and "experienced" observers. If the observed area of a sunspot exceeded the true threshold sunspot area, it was concluded that this sunspot would have been large enough to be seen with the unaided eye by either an "average" or "experienced" ancient observer in East Asia, depending on which of the various threshold areas was exceeded. If the sunspot was also within $\pm 50°$ of heliographic longitude with respect to the central meridian (i.e. within the dotted lines shown in Fig. 1a of the earlier paper), it was further concluded that the sunspot de-

fined an active solar region near to the central meridian immediately before the corresponding Japanese auroral observation(s). Essentially the same procedure is now used to investigate the presence of large sunspots near the central solar meridian at the times of modern geomagnetic storms.

5   The presence of large sunspots immediately before major geomagnetic storms

As noted in Sect. 4, the apparent semi-diameter of the Sun varies during the course of the year. Although this annual variation is small (amounting to a difference of only 32 arc s between January and July), it is allowed for in the present investigation because the projected threshold areas (measured in millionths of the solar disk), corresponding to a "constant" threshold dimension quoted in arc seconds (see Sect. 4), do vary slightly during the year (Table 1). The semi-diameter of the Sun has been calculated using a simple computer program, which is based on the principal terms in the solar theory developed long ago by Newcomb (1898). Purely elliptical motion of the Earth in its orbit is assumed and no allowance is made for planetary terms. The adopted semi-diameter at unit distance is taken to be 961.18 arc s, which is an enhanced value that includes an allowance for irradiation (Explanatory Supplement to The Astronomical Almanac, 1992). (It is standard practice to use a smaller value of the semi-diameter at unit distance (959.63″) in the calculation of eclipses.) The adopted value (961.18″) is that used in "The Nautical Almanac" for years immediately preceding 1960 and differs from that used before 1960 (961.50″) in "The American Ephemeris" because of a different allowance for irradiation.

A sample check against data in "The Astronomical Ephemeris" for the penultimate year (1975) of the RGO programme of solar observations indicates that when computations are made using the simple computer program there is a typical error of about 0.1 arc s (i.e. about 1 part in 10 000) in the solar semi-diameter: such an error is insignificant in the context of the present study. In addition, a more comprehensive computer program, which includes planetary terms, has been used to check the accuracy of the simple program. The magnitude of the discrepancy between the results obtained by the two programs is less than 0.11 arc s throughout the interval 1874–1976, which is again insignificant in the context of present study. However, owing to the ellipticity of the Earth's orbit, the solar semi-diameter can change by up to 0.27 arc s in 24 h (notably in April and October). Therefore, in order to calculate true threshold areas accurately, it is important to input the time (UT) of the solar photograph, when known. On days when no sunspots were observed on the solar disk and no time is recorded in the original digital dataset, the time of the photograph is arbitrarily assumed to be 12:00 UT.

Of course, the accuracy quoted in the previous paragraph is partly spurious. The "constant" threshold angular

dimensions quoted previously for the detection of sunspots by "average" and "experienced" observers (namely 15 and 41 arc s, and 25 arc s, respectively) are characteristic values not absolute values. Moreover, the semi-diameter of the Sun was used in the measurement of sunspot areas on the solar plates (photo-heliograms). All publications of the Royal Greenwich Observatory that discuss the measurement of sunspot areas on the photographs refer to the "tabular semi-diameter of the Sun in arc" without further explanation. It is assumed here that these tabular values of the semi-diameter were taken from "The Nautical Almanac" or "The Astronomical Ephemeris", since it seems unlikely that semi-diameters would have been calculated again solely to derive sunspot areas. Even in the earliest years, values of the semi-diameter published in "The Nautical Almanac" exceed those obtained from the computer program by less than 1 arc s. From the beginning of the twentieth century, the magnitude of the discrepancy is less than 0.25 arc s.

Table 1 shows the characteristic variation of the threshold sunspot areas during the course of the year. Approximate numerical values of these threshold sunspot areas are presented for the minimum, mean and maximum distances of the Sun from the Earth. Projected umbral and whole-spot (umbral + penumbral) threshold areas, expressed in millionths of the solar disk, are given for both "average" and "experienced" sunspot observers. For brevity, the symbols U_0, P_0 and W_0 ($=U_0+P_0$) are used to denote the umbral, penumbral and whole-spot (= umbral + penumbral) threshold areas. The uncertainties associated with the threshold areas, which are presented in [square] parentheses, are estimates based on a characteristic uncertainty of $\pm10\%$ in the threshold sunspot dimensions quoted in arc seconds. This characteristic uncertainty is consistent with the results found by Keller and Friedli (1992) in a case study involving 10 experienced sunspot observers, using the mean visibility limit of the three best observers. These authors concluded that the determining factor for detecting a sunspot with the unaided eye is the contrast ratio between the brightness of the (unresolved) combination of umbra and penumbra and the brightness of the surrounding photosphere. It should be noted that the uncertainties ($\sim10\%$) in the threshold sunspot dimensions are much larger than the maximum uncertainty ($\sim0.1\%$) in the semi-diameter of the Sun. However, it is clear from the numbers presented in Table 1 that the contribution to changes in threshold sunspot areas arising from the annual variation in the apparent semi-diameter of the Sun (i.e. 32 arc s) is just significant.

As noted in Sect. 4, the condition for the detection of the historical occurrence of a geomagnetic storm is also based on the assumption that the energetic solar feature producing the historical geomagnetic storm must have occurred when the associated sunspot was within ±4 days (or about $\pm50°$ of heliographic longitude) of the central solar meridian. It is convenient to introduce the symbol Λ to denote longitudinal distance from the central solar meridian, which is measured

in degrees. Both the technique for the identification of an historical geomagnetic storm (Willis et al., 2005), and the subsequent verification of the technique using modern Japanese auroral observations (Willis et al., 2006), require Λ to satisfy the condition $-50° < \Lambda < +50°$. The numbers and percentages of major geomagnetic storms in the interval 1874–1976 that satisfy the various criteria for sunspot visibility, specified in terms of the quantities Λ, U, W, U_0 and W_0, are presented in Table 2, where the additional symbols S, A, a, F and f are used to signify "success" (S), "ambiguity" (A or a) and "failure" (F or f), respectively.

The exact definitions of the symbols S, A, a, F and f are given explicitly in the footnotes to Table 2. There are two types of "ambiguity" and "failure" for an "average" sunspot observer. In particular, the symbol "A" signifies $U > U_0$ and $W < W_0$, whereas the symbol "a" signifies $U < U_0$ and $W > W_0$. Likewise, the symbol "F" signifies $U < U_0$ and $W < W_0$, whereas the symbol "f" signifies $\Lambda \leq -50°$ or $\Lambda \geq +50°$ (which is a "failure" irrespective of the values of U and W). Similar definitions apply to an "experienced" sunspot observer, although ambiguities do not arise in this case. For brevity, the symbol $\forall$ (from logic and set theory) is used to signify "for all values of" or, more accurately, "irrespective of the values of" the qualified variables (i.e. U and W). The changes in the numbers of major geomagnetic storms that satisfy the various sunspot visibility criteria, arising from characteristic uncertainties of $\pm10\%$ in threshold sunspot dimensions in arc seconds, are given in [square] parentheses.

It is clear from the numbers presented in Table 2 that an "experienced" sunspot observer achieves a success rate (unadjusted) of almost 90% (87.5%). Since no sunspot data are available for 23 of these 1074 major geomagnetic storms, the adjusted success rate is indeed very close to 90% (89.4%). Even an "average" sunspot observer achieves an unadjusted success rate greater than 70% (71.2%). Moreover, if the two ambiguous cases (A and a) presented in Table 2 are regarded as successes, and allowance is again made for the fact that no sunspot data are available for 23 of these major geomagnetic storms, the adjusted success rate for an "average" sunspot observer just exceeds 80%.

The numbers in [square] parentheses in Table 2 show the variations in the number of major geomagnetic storms satisfying the various sunspot visibility criteria if the threshold sunspot dimensions (in arc seconds) are assumed to have characteristic uncertainties of $\pm10\%$. It should be noted that there is no change in the number of cases that fail to satisfy the condition $-50° < \Lambda < +50°$ and that the cases which do satisfy this condition are merely redistributed among the different sunspot visibility criteria, as is obvious logically. It follows from the numbers presented in Table 2 that, if the threshold sunspot dimensions are increased by 10%, an "experienced" sunspot observer would still achieve an adjusted success rate of 88% and an "average" sunspot observer would achieve an adjusted success rate of 68%, even if the

Table 2. Numbers and percentages of major geomagnetic storms in the interval 1874–1976 for which the different sunspot visibility criteria defined in Sect. 5 are satisfied. In the case of "average" sunspot observers, the five conditions (sets of inequalities or conditions) defined in the footnotes to the table are considered sequentially for each sunspot group on the solar disk, during the six-day interval immediately before the onset of each major geomagnetic storm. Similarly, in the case of "experienced" sunspot observers, the three conditions (single inequalities) defined in the footnotes are considered sequentially. For each major geomagnetic storm, a single success (S), ambiguity (A or a) or failure (F or f) is recorded (accumulated in the table) as soon as one of the sequential conditions is satisfied. The symbols U_0 and W_0 ($=U_0+P_0$) are again used to denote the umbral and whole-spot threshold areas and Λ denotes angular longitudinal distance from the central solar meridian. For brevity, the symbol $\forall(U, W)$ signifies "for all values of U and W" (or "irrespective of the values of U and W"); similarly, $\forall(W)$ signifies "for all values of W" (or "irrespective of the value of W"). The variations in the number of major geomagnetic storms that satisfy the different sunspot visibility criteria, associated with characteristic uncertainties of $\pm10\%$ in the threshold sunspot dimensions in arc seconds, are presented in [square] parentheses.

Average sunspot observers			
Sunspot visibility criterion	Number of major geomagnetic storms	Percentage of total number of storms	Variation in number of storms [$\pm10\%$ threshold sunspot dimensions]
S (Success)	765	71.2	[−49, +53]
A (Ambiguity)	70	6.5	[+0, −15]
a (ambiguity)	9	0.8	[+2, −6]
F (Failure)	199	18.5	[+47, −32]
f (failure)	8	0.8	[+0, −0]
No sunspot data	23	2.1	–
Total	1074	99.9	–
Experienced sunspot observers			
Sunspot visibility criterion	Number of major geomagnetic storms	Percentage of total number of storms	Variation in number of storms [$\pm10\%$ threshold sunspot dimensions]
S (Success)	940	87.5	[−14, +25]
F (Failure)	103	9.6	[+14, −25]
f (failure)	8	0.8	[+0, −0]
No Sunspot Data	23	2.1	–
Total	1074	100.0	–

Definitions: The sunspot visibility criteria (S, A, a, F, and f) for "average" observers are defined as follows: "S" implies $-50°<\Lambda<+50°$, $U>U_0$ (avg) and $W>W_0$ (avg); "A" implies $-50°<\Lambda<+50°$, $U>U_0$ (avg) and $W<W_0$ (avg); "a" implies $-50°<\Lambda<+50°$, $U<U_0$ (avg) and $W>W_0$ (avg); "F" implies $-50°<\Lambda<+50°$, $U<U_0$ (avg) and $W<W_0$ (avg); and "f" implies $\Lambda\leq-50°$ or $\Lambda\geq+50°$, $\forall(U, W)$. Similarly, the sunspot visibility criteria for "experienced" observers are defined as follows: "S" implies $-50°<\Lambda<+50°$ and $W>W_0$ (exp); "F" implies $-50°<\Lambda<+50°$ and $W<W_0$ (exp); and "f" implies $\Lambda\leq-50°$ or $\Lambda\geq+50°$, $\forall(W)$.

ambiguous cases (A and a) are ignored. If the threshold sunspot dimensions are increased by 20%, the corresponding adjusted success rates are 86% and 63%. Likewise, the adjusted success rates do not depend markedly on the acceptable range of longitudes with respect to the central solar meridian, namely $-\Lambda_0<\Lambda<+\Lambda_0$, provided that $\Lambda_0\geq30°$, a condition that is clearly satisfied by the representative value $\Lambda_0=50°$ used in this investigation and in the previous studies (Willis et al., 2005, 2006). Obviously, in the limit $\Lambda_0\rightarrow0$, the success rate tends to zero.

6   Discussion

The results presented in this paper indicate that at least one sunspot large enough to be seen with the unaided eye was reasonably close to the central solar meridian ($-50°<\Lambda<+50°$) during an interval extending over 1–6 days prior to the onset time of most of the major geomagnetic storms ($AA*>60$ nT) in the interval 1874–1976 (Allen, 1982; Coffey and Erwin, 2001; ftp://ftp.ngdc.noaa.gov/STP/ GEOMAGNETIC_DATA/AASTAR/aastar.lst.v7). In particular, the success rate for an "experienced" sunspot observer would have been almost 90% and the success rate for an "average" sunspot observer would have been about 70%. In a similar investigation, using Japanese auroral observations in the interval 1957–2004 (Willis et al., 2006), the corresponding success rates for "experienced" and "average" sunspot observers were found to be 97% and 80%. Both investigations confirm the validity of the technique developed by Willis et al. (2005) to identify historical occurrences of intense geomagnetic storms, which is based on finding approximately coincident observations of sunspots and aurorae recorded in East Asian histories.
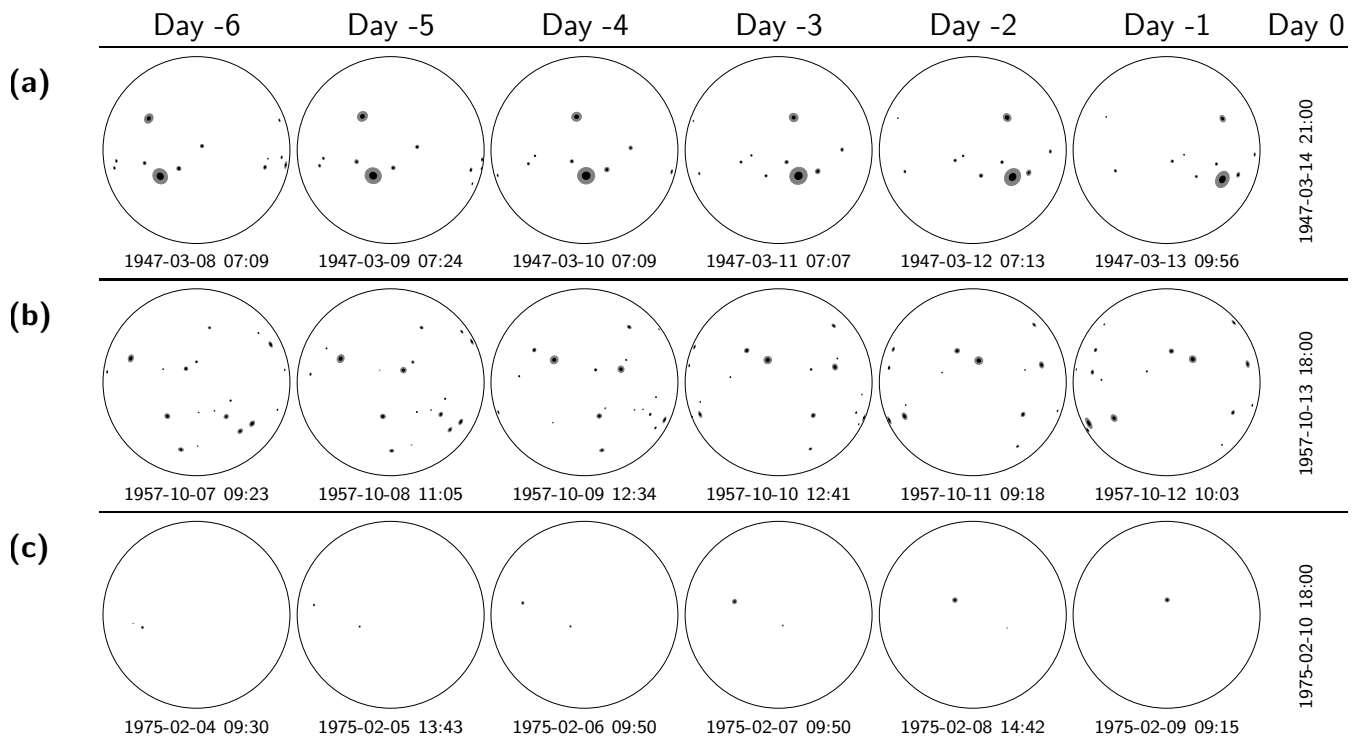
Fig. 1. Reconstructed solar images for the six-day intervals immediately before the major geomagnetic storms that commenced on: **(a)** 1947 March 14; **(b)** 1957 October 13; and **(c)** 1975 February 10.

As noted in the introduction, the method used to detect sunspots large enough to be seen with the unaided eye has to be semi-automated because of the large number (1074) of major geomagnetic storms in the interval 1874 April 17–1976 December 31. Similarly, it is impracticable to show all the solar images, so statistical results have to be presented instead (Table 2). However, it is instructive to present a few illustrations of sunspots on the solar disk for the six days before the day of the onset of a major geomagnetic storm. Figure 1 shows reconstructed solar images (see Willis et al., 1996) for the six-day intervals immediately before the three major geomagnetic storms that commenced on 1947 March 14, 1957 October 13 and 1975 February 10. The date and time (UT) of the onset of each geomagnetic storm is presented at the right-hand side of the figure (Day 0) and the date and time of each solar observation is presented immediately below the corresponding solar image (Day -6 to Day -1). For consistency, the format of Fig. 1 (and Fig. 2) is exactly the same as that employed for the figures presented in the earlier paper on the presence of large sunspots near the central solar meridian at the times of modern Japanese auroral observations (Willis et al., 2006). All three examples of major geomagnetic storms shown in Fig. 1 represent an overall success (S) in terms of the various classification criteria introduced in Sect. 5 and employed in Table 2 (see footnotes). These classifications are: success (S), ambiguity (A or a) and failure (F or f). Therefore, at least one sunspot

large enough to be seen with the unaided eye by both "average" and "experienced" solar observers is present on the solar disk for at least one of the six days immediately before the day of the onset of each of the three geomagnetic storms depicted in Fig. 1, which counts as an overall success (S).

The three panels in Fig. 1 can also be discussed individually on a daily basis. Panel (a) shows a very large (giant) sunspot and a large sunspot on the solar disk throughout the six-day interval before the geomagnetic storm that commenced on 1947 March 14. Panel (b) shows at least one large sunspot on the solar disk throughout the six-day interval before the geomagnetic storm that commenced on 1957 October 13. The large sunspots on the solar disk before these two storms can be detected easily by both "average" and "experienced" sunspot observers. Panel (c) shows one sunspot just large enough to be detected by both "average" and "experienced" observers for the two days immediately before the geomagnetic storm that commenced on 1975 February 10. An "experienced" observer can also detect a sunspot on the third and fourth days before the onset of this storm (S), whereas for an "average" observer the detection of a sunspot is ambiguous on the third day before the storm (a: $U < U_0$, $W > W_0$) and impossible (failure) on the fourth day before the storm (F: $U < U_0$, $W < W_0$). Neither an "average" nor an "experienced" sunspot observer can detect a sunspot on the fifth and sixth days before the onset of this geomagnetic storm (F: $U < U_0$, $W < W_0$).
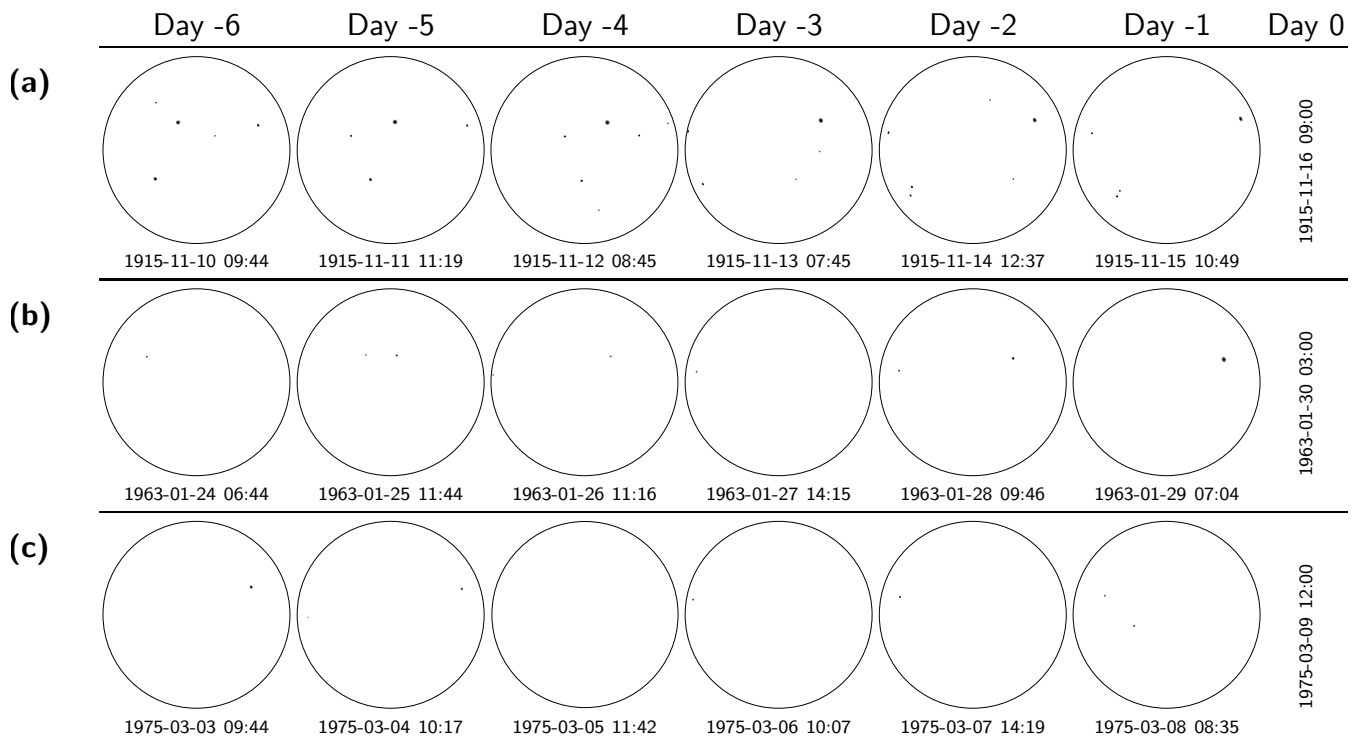
Fig. 2. Reconstructed solar images for the six-day intervals immediately before the major geomagnetic storms that commenced on: **(a)** 1915 November 16; **(b)** 1963 January 30; and **(c)** 1975 March 9. No sunspots were present on the solar disk on 1975 March 5 (and hence no information is stored in the sunspot digital dataset for this particular day).

Similarly, Fig. 2 shows reconstructed solar images for the six-day intervals immediately before the three major geomagnetic storms that commenced on 1915 November 16, 1963 January 30 and 1975 March 9. These particular storms have been chosen deliberately to illustrate three different situations that are not an overall success (S) from the viewpoint of both "average" and "experienced" sunspot observers. The three panels in Fig. 2 can again be discussed individually on a daily basis. Panel (a) shows a sunspot large enough to be seen by only an "experienced" observer, but more than 50° from the central meridian (f: $\Lambda \geq +50°$), on the day immediately before the geomagnetic storm that commenced on 1915 November 16. On the second to sixth days before this storm, an "experienced" observer is capable of detecting a sunspot (S: $W > W_0$), whereas for an "average" observer the detection of a sunspot is ambiguous throughout these five days (A: $U > U_0$, $W < W_0$). Panel (b) shows a sunspot large enough to be seen by an "experienced" observer on the day immediately before the geomagnetic storm that commenced on 1963 January 30, whereas for an "average" observer the detection of a sunspot on this day is ambiguous (a: $U < U_0$, $W > W_0$). On the second, fourth, fifth and sixth days before the onset of this storm, there are no sunspots large enough to be seen by either "average" or "experienced" observers (F: $U < U_0$, $W < W_0$); on the third day before this storm, the only sunspot on the solar disk is more than 50° from the central meridian

(f: $\Lambda \leq -50°$). Panel (c) shows that there are no sunspots on the solar disk large enough to be seen by either "average" or "experienced" observers on the first and sixth days before the geomagnetic storm that commenced on 1975 March 9. On the second, third and fifth days before the storm, there are no sunspots within 50° of the central meridian (f: $\Lambda \leq -50°$ or $\Lambda \geq +50°$). No sunspots were observed on the solar disk on the fourth day before the storm. (Therefore, this particular day should really be regarded as separate type of "failure" because no information is stored in the digital sunspot dataset on days when no sunspots were observed on the solar disk.)

A success, ambiguity or failure symbol (S, A, a, F or f) is assigned to every sunspot on the solar disk for each of the six days preceding each major geomagnetic storm in the interval 1874–1976; this is done separately for "average" and "experienced" sunspot observers. For both types of sunspot observer, an overall classification symbol is then assigned to each storm by selecting the highest-ranked (sunspot) symbol within the six-day period, if these symbols are ranked in the strict priority order S, A, a, F, and f. For 23 of these six-day intervals, no RGO sunspot data are available for any day, so the number of major geomagnetic storms that can be given such an overall classification is 1051, which accounts for the use of the term "adjusted success rate" in Sect. 5. The numbers of major geomagnetic storms in the various categories are presented in Table 2.

Examples of major geomagnetic storms that occur when the corresponding solar photographs show sunspots too small to be detected with the unaided eye (or even show the total absence of sunspots), as exemplified in panels (b) and (c) of Fig. 2, require further consideration. The 23 major geomagnetic storms for which no sunspot information is archived in the printed RGO publications (Sect. 5 and Table 2) – on all six days before the onset of each storm – occur near sunspot minimum, without exception. This suggests that the absence of archived information correctly implies the absence of sunspots. Furthermore, by considering the dates of major geomagnetic storms that immediately precede or follow these 23 geomagnetic storms, it is evident that some of these particular storms are examples of recurrent geomagnetic storms. Recurrent storms are normally associated with co-rotating solar wind streams or co-rotating interaction regions (Crooker and Cliver, 1994; Tsurutani et al., 2006). In particular, it is known that solar-wind fast streams emanating from coronal holes cause recurrent, moderate intensity geomagnetic activity at the Earth. Moreover, co-rotating interaction regions (CIRs) are regions of intense magnetic field formed when high-speed solar wind streams overtake slow solar wind streams as they propagate away from the Sun. Geomagnetic storms produced by co-rotating interaction regions are generally weaker than those produced by coronal mass ejections (Tsurutani et al., 2006; Alves et al., 2006; Denton et al., 2006; Borovsky and Denton, 2006; Richardson et al., 2006), although there are some notable exceptions (Richardson et al., 2006). However, a detailed discussion of the different types of solar activity that result in recurrent and non-recurrent geomagnetic storms is well beyond the intended scope of the present paper.

Of course, there are numerous examples of large sunspot groups observed near the central solar meridian that are not accompanied by either a geomagnetic storm or an auroral display. There may be several different reasons for the lack of any concomitant geomagnetic or auroral activity. In many cases, transient solar activity associated with a large sunspot group does not occur when the group is near the central solar meridian and hence does not result in a coronal mass ejection (CME) that is directed towards the Earth. Moreover, even if the CME is directed towards the Earth, the severity of the resulting geomagnetic storm depends crucially on the amount of southward-directed magnetic flux (B_z) carried to the Earth (Gonzalez et al., 1999; Richardson et al., 2006; Zhang et al., 2007a). In the limit of negligible southward-directed magnetic flux impinging on the Earth's magnetosphere, a major geomagnetic storm would not be generated. Although this limiting situation would be rare, since the interplanetary magnetic field varies considerably with time, it is relatively easy to provide physical explanations for solar activity not resulting in geomagnetic or auroral activity. Conversely, it is rather more difficult to explain the small number of major geomagnetic storms that are apparently not associated with any obvious manifestation of solar activity.

It should be noted that a number of assumptions have been made in this investigation. For example, assumptions have been made about the threshold dimensions for the detection of sunspots with the unaided eye by both "average" and "experienced" observers (Sect. 4), although allowance has been made for ±10% uncertainties in these dimensions (Sect. 5). Similarly, some uncertainty exists regarding the value of the semi-diameter of the Sun used to analyse the RGO photo-heliograms (Sect. 5), although it has been shown that this particular uncertainty is insignificant. Likewise, the main calculations have been performed on the assumption that a sunspot can only be associated meaningfully with a major geomagnetic storm if the angular distance (Λ) of the sunspot from the central solar meridian satisfies the condition $-50° < \Lambda < +50°$ (Sect. 4). However, it has been found that this assumption is acceptable provided that $\Lambda_0 \geq 30°$ in the inequality $-\Lambda_0 < \Lambda < +\Lambda_0$. In defining the six-day interval immediately before a major geomagnetic storm, it is assumed that the onset time of the storm is the beginning of the appropriate the 3-h interval of the $AA*$ magnetic index. This assumption introduces a timing uncertainty because the time of the RGO solar observation on the "first" day before the onset of the geomagnetic storm is taken to be as close as possible to, but greater than, the limiting value of 17.5 h (Sect. 4). Furthermore, on days for which no sunspots exist on the solar disk, no information is stored in the digital sunspot dataset. In such cases, it is assumed for determinateness that the solar observations were actually made at 12:00 UT (Sect. 5). Despite these largely inevitable assumptions, the results presented in Table 2 provide conclusive statistical evidence for the presence of large sunspots near the central solar meridian at the times of major geomagnetic storms.

7 Conclusions

The present paper provides further support for the validity of the technique developed by Willis et al. (2005) for the identification of historical occurrences of intense geomagnetic storms, which is based on finding approximately coincident observations of sunspots and aurorae recorded in East Asian histories. Previously, Willis et al. (2006) provided direct confirmation of the validity of this technique using modern Japanese auroral observations in the interval 1957–2004. The new study reported here utilises a list of major geomagnetic storms that occurred in the interval 1868–2008 to investigate the presence or absence of large sunspots near the central solar meridian during the shorter interval 1874–1976, which is determined solely by the availability of homogeneous sunspot data acquired by the Royal Greenwich Observatory. The use of information on major geomagnetic storms, rather than modern auroral observations from Japan, provides a less direct corroboration of the technique for detecting historical occurrences of intense geomagnetic storms, if only because geomagnetic storms do not necessarily produce

auroral displays over East Asia. Nevertheless, the present study provides further corroboration of the validity of the original technique for the identification of historical occurrences of intense geomagnetic storms (Willis et al., 2005).

As noted previously, this further corroboration is important because early unaided-eye observations of sunspots and aurorae provide the only possible means of identifying individual geomagnetic storms during the greater part of the past two millennia. Moreover, in terms of identifying historical occurrences of intense geomagnetic storms, it is entirely plausible that the success rates for modern Japanese auroral observations should be higher than those for modern geomagnetic storms, since it is known that not all geomagnetic storms generate auroral displays in East Asia.

Finally, it should be emphasised again that it is not being claimed in this study or in the previous investigation by Willis et al. (2006) that large sunspots near the central solar meridian cause geomagnetic storms and low-latitude auroral displays. There are numerous examples of large sunspots near the central solar meridian that are clearly not associated with either a geomagnetic storm or an auroral display. However, sunspots that are in the vicinity of the central solar meridian and large enough to be seen with the unaided eye appear to indicate potential (or latent) solar activity that is capable of producing an intense geomagnetic storm and a concomitant auroral display at low geomagnetic latitudes. The procedure for identifying the historical occurrence of a geomagnetic storm (Willis et al., 2005) depends on the approximate coincidence of a large sunspot in the vicinity of the central solar meridian and a conspicuous auroral display at low geomagnetic latitudes (both visible with the unaided eye). Therefore, large sunspots that are not associated with a geomagnetic storm and a concomitant auroral display are never identified by the selection procedure for historical occurrences of intense geomagnetic storms.

References

Allen, J. H.: Some commonly used magnetic activity indices: their derivation, meaning and use, in: Proceedings of the Workshop on Satellite Drag, edited by: Joselyn, J., Boulder, Colorado, 114–134, 1982.

Alves, M. V., Echer, E., and Gonzalez, W. D.: Geoeffectiveness of corotating interaction regions as measured by D_{st} index, J. Geophys. Res., 111, A07S05, doi:10.1029/2005JA011379, 2006.

Berdichevsky, D. B., Farrugia, C. J., Thompson, B. J., Lepping, R. P., Reames, D. V., Kaiser, M. L., Steinberg, J. T., Plunkett, S. P., and Michels, D. J.: Halo-coronal mass ejections near the 23rd solar minimum: lift-off, inner heliosphere, and in situ (1 AU) signatures, Ann. Geophys., 20, 891–916, 2002, http://www.ann-geophys.net/20/891/2002/.

Borovsky, J. E. and Denton, M. H.: Differences between CME-driven storms and CIR-driven storms, J. Geophys. Res., 111, A07S08, doi:10.1029/2005JA011447, 2006.

Cane, H. V. and Richardson, I. G.: Interplanetary coronal mass ejections in the near-Earth solar wind during 1996–2002, J. Geophys. Res., 108(A4), 1156, doi:10.1029/2002JA009817, 2003.

Cane, H. V., Richardson, I. G., and St. Cyr, O. C.: Coronal mass ejections, interplanetary ejecta and geomagnetic storms, Geophys. Res. Lett., 27, 3591–3594, 2000.

Carrington, R. C.: Description of a singular appearance seen in the Sun on September 1, 1859, Mon. Not. R. Astron. Soc., 20, 13–15, 1860.

Clilverd, M. A., Clark, T. D. G., Clarke, E., and Rishbeth, H.: Increased magnetic storm activity from 1868 to 1995, J. Atmos. Sol.-Terr. Phys., 60, 1047–1056, 1998.

Clilverd, M. A., Clarke, E., Ulich, T., Linthe, J., and Rishbeth, H.: Reconstructing the long-term *aa* index, J. Geophys. Res., 110, A07205, doi:10.1029/2004JA010762, 2005.

Coffey, H. E. and Erwin, E. H.: When do the geomagnetic aa and Ap indices disagree?, J. Atmos. Sol.-Terr. Phys., 63, 551–556, 2001.

Crooker, N. U. and Cliver, E. W.: Postmodern view of M-regions, J. Geophys. Res., 99, 23383–23390, 1994.

Denton, M. H., Borovsky, J. E., Skoug, R. M., Thomsen, M. F., Lavraud, B., Henderson, M. G., McPherron, R. L., Zhang, J. C., and Liemohn, M. W.: Geomagnetic storms driven by ICME-and CIR-dominated solar wind, J. Geophys. Res., 111, A07S07, doi:10.1029/2005JA011436, 2006.

Explanatory Supplement to the Astronomical Almanac: University Science Books, Mill Valley, California, edited by: Seidelmann, P. K., 1992.

Foster, S. S.: Reconstruction of solar irradiance variations, for use in studies of global climate change: Application of recent SoHO observations with historic data from the Greenwich Observatory, PhD Thesis, School of Physics and Astronomy, University of Southampton, 2004.

Gonzalez, W. D., Tsurutani, B. T., and Clúa de Gonzalez, A. L.: Interplanetary origin of geomagnetic storms, Space Sci. Rev., 88, 529–562, 1999.

Gopalswamy, N., Yashiro, S., Michalek, G., Xie, H., Lepping, R. P., and Howard, R.A.: Solar source of the largest geomagnetic storm of cycle 23, Geophys. Res. Lett., 32, L12S09, doi:10.1029/2004GL021639, 2005.

Gopalswamy, N., Yashiro, S., and Akiyama, S.: Geoeffectiveness of halo coronal mass ejections, J. Geophys. Res., 112, A06112, doi:10.1029/2006JA012149, 2007.

Hodgson, R.: On a curious appearance seen in the Sun, Mon. Not. R. Astron. Soc., 20, 15–16, 1860.

Howse, H. D.: Greenwich Observatory: The Royal Observatory at Greenwich and Herstmonceux 1675–1976, Volume 3: Buildings and Instruments, Taylor and Francis, London, 1975.

Hudson, H. S., Lemen, J. R., St. Cyr, O. C., Sterling, A. C., and Webb, D. F.: X-ray coronal changes during halo CMEs, Geo-

phys. Res. Lett., 25, 2481–2484, 1998.

Jarvis, M. J.: Observed tidal variation in the lower thermosphere through the 20th century and the possible implication of ozone depletion, J. Geophys. Res., 110, A04303, doi:10.1029/2004JA010921, 2005.

Kang, Seung-Mi, Moon, Y.-J., Cho, K.-S., Kim, Yeon-Han, Park, Y. D., Baek, Ji-Hye, and Chang, Heon-Young: Coronal mass ejection geoeffectiveness depending on field orientation and interplanetary coronal mass ejection classification, J. Geophys. Res., 111, A05102, doi:10.1029/2005JA011445, 2006.

Keller, H. U. and Friedli, T. K.: Visibility limit of naked-eye sunspots, Q. J. Roy. Astron. Soc., 33, 83–89, 1992.

Kim, R.-S., Cho, K.-S., Moon, Y.-J., Kim, Y.-H., Yi, Y., Dryer, M., Bong, Su-Chan, and Park, Y.-D.: Forecast evaluation of the coronal mass ejection (CME) geoeffectiveness using halo CMEs from 1997 to 2003, J. Geophys. Res., 110, A11104, doi:10.1029/2005JA011218, 2005.

Mayaud, P. N.: The *aa* indices: a 100-year series characterizing the magnetic activity, J. Geophys. Res., 77, 6870–6874, 1972.

Mayaud, P. N.: A hundred year series of geomagnetic data, 1868–1967, indices *aa*, Storm sudden commencements, IAGA Bulletin No. 33, IUGG Publications Office, Paris, 1973.

Mayaud, P. N.: Derivation, Meaning, and Use of Geomagnetic Indices, Geophysical Monograph 22, American Geophysical Union, Washington, D.C., 1980.

Mursula, K. and Martini, D.: Centennial increase in geomagnetic activity: Latitudinal differences and global estimates, J. Geophys. Res., 111, A08209, doi:10.1029/2005JA011549, 2006.

Newcomb, S.: Tables of the Motion of the Earth on its Axis and Around the Sun, Astronomical Papers of the American Ephemeris and Nautical Almanac, Volume VI, Part 1, pp. 1–169, Washington, D.C., 1898.

Newton, H. W.: The Face of the Sun, Penguin Books Ltd, Harmondsworth, Middlesex, 1958.

Richardson, I. G., Webb, D. F., Zhang, J., Berdichevsky, D. B., Biesecker, D. A., Kasper, J. C., Kataoka, R., Steinberg, J. T., Thompson, B. J., Wu, C.-C., and Zhukov, A. N.: Major geomagnetic storms ($D_{st} \leq -100$ nT) generated by corotating interaction regions, J. Geophys. Res., 111, A07S09, doi:10.1029/2005JA011476, 2006.

Rouillard, A. P., Lockwood, M., and Finch, I.: Centennial changes in the solar wind speed and in the open solar flux, J. Geophys. Res., 112, A05103, doi:10.1029/2006JA012130, 2007.

Schwenn, R., Dal Lago, A., Huttunen, E., and Gonzalez, W. D.: The association of coronal mass ejections with their effects near the Earth, Ann. Geophys., 23, 1033–1059, 2005, http://www.ann-geophys.net/23/1033/2005/.

Shiokawa, K., Ogawa, T., and Kamide, Y.: Low-latitude auroras observed in Japan: 1999–2004, J. Geophys. Res., 110, A05202, doi:10.1029/2004JA010706, 2005.

Srivastava, N. and Venkatakrishnan, P.: Solar and interplanetary sources of major geomagnetic storms during 1996–2002, J. Geophys. Res., 109, A10103, doi:10.1029/2003JA010175, 2004.

Svalgaard, L. and Cliver, E. W.: Interhourly variability index of geomagnetic activity and its use in deriving the long-term variation of solar wind speed, J. Geophys. Res., 112, A10111, doi:10.1029/2007JA012437, 2007.

Svalgaard, L., Cliver, E. W., and Le Sager, P.: IHV: a new long-term geomagnetic index, Adv. Space Res., 34, 436–439, 2004.

Tsurutani, B. T., Gonzalez, W. D., Gonzalez, A. L. C., Guarnieri, F. L., Gopalswamy, N., Grande, M., Kamide, Y., Kasahara, Y., Lu, G., Mann, I., McPherron, R., Soraas, F., and Vasyliunas, V.: Corotating solar wind streams and recurrent geomagnetic activity: A review, J. Geophys. Res., 111, A07S01, doi:10.1029/2005JA011273, 2006.

Tsurutani, B. T., Echer, E., Guarnieri, F. L., and Kozyra, J. U.: CAWSES November 7–8, 2004, superstorm: Complex solar and interplanetary features in the post-solar maximum phase, Geophys. Res. Lett., 35, L06S05, doi:10.1029/2007GL031473, 2008.

Webb, D. F., Cliver, E. W., Crooker, N. U., St. Cyr, O. C., and Thompson, B. J.: Relationship of halo coronal mass ejections, magnetic clouds, and magnetic storms, J. Geophys. Res., 105(A4), 7491–7508, 2000.

Willis, D. M., Davda, V. N., and Stephenson, F. R.: Comparison between oriental and occidental sunspot observations, Q. J. Roy. Astron. Soc., 37, 189–229, 1996.

Willis, D. M., Armstrong, G. M., Ault, C. E., and Stephenson, F. R.: Identification of possible intense historical geomagnetic storms using combined sunspot and auroral observations from East Asia, Ann. Geophys., 23, 945–971, 2005, http://www.ann-geophys.net/23/945/2005/.

Willis, D. M., Henwood, R., and Stephenson, F. R.: The presence of large sunspots near the central solar meridian at the times of modern Japanese auroral observations, Ann. Geophys., 24, 2743–2758, 2006, http://www.ann-geophys.net/24/2743/2006/.

Zhang, J., Richardson, I. G., Webb, D. F., Gopalswamy, N., Huttunen, E., Kasper, J. C., Nitta, N. V., Poomvises, W., Thompson, B. J., Wu, C.-C., Yashiro, S., and Zhukov, A. N.: Solar and interplanetary sources of major geomagnetic storms ($D_{st} \leq -100$ nT) during 1996–2005, J. Geophys. Res., 112, A10102, doi:10.1029/2007JA012321, 2007a.

Zhang, J., Richardson, I. G., Webb, D. F., Gopalswamy, N., Huttunen, E., Kasper, J., Nitta, N. V., Poomvises, W., Thompson, B. J., Wu, C.-C., Yashiro, S., and Zhukov, A. N.: Correction to "Solar and interplanetary sources of major geomagnetic storms ($D_{st} \leq -100$ nT) during 1996–2005", J. Geophys. Res., 112, A12103, doi:10.1029/2007JA012891, 2007b.